ACS APPLIED MATERIALS & INTERFACES

Research Article

www.acsami.org

Fluorescent Molecular Rotor-in-Paraffin Waxes for Thermometry and Biometric Identification

Young-Jae Jin,[†] Rubal Dogra,[‡] In Woo Cheong,[‡] and Giseop Kwak*[,†]

[†]School of Applied Chemical Engineering, Polymer Science and Engineering, Kyungpook National University, 1370 Sankyuk-dong, Buk-ku, Daegu 702−701, Korea

[‡]School of Applied Chemical Engineering, Applied Chemistry, Kyungpook National University, 1370 Sankyuk-dong, Buk-ku, Daegu 702-701, Korea

Supporting Information

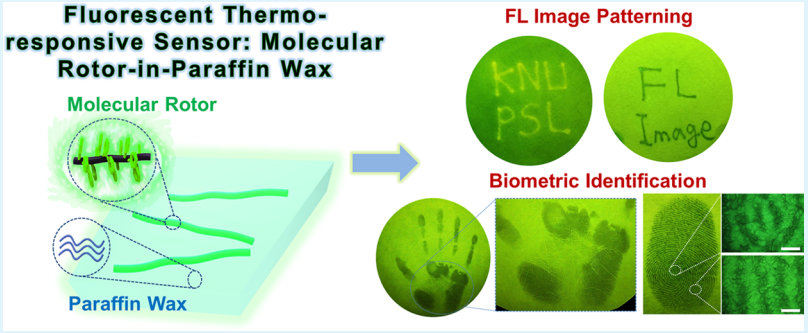

ABSTRACT: Novel thermoresponsive sensor systems consisting of a molecular rotor (MR) and paraffin wax (PW) were developed for various thermometric and biometric identification applications. Polydiphenylacetylenes (PDPAs) coupled with long alkyl chains were used as MRs, and PWs of hydrocarbons having 16−20 carbons were utilized as phase-change materials. The PDPAs were successfully dissolved in the molten PWs and did not act as an impurity that prevents phase transition of the PWs. These PDPA-in-PW hybrids had almost the same enthalpies and phase-transition temperatures as the corresponding pure PWs. The hybrids exhibited highly reversible fluorescence (FL) changes at the critical temperatures during phase transition of the PWs. These hybrids were impregnated into common filter paper in the molten state by absorption or were encapsulated into urea resin to enhance their mechanical integrity and cyclic stability during repeated use. The wax papers could be utilized in highly advanced applications including FL image writing/erasing, an array-type thermo-indicator, and fingerprint/palmprint identification. The present findings should facilitate the development of novel fluorescent sensor systems for biometric identification and are potentially applicable for biological and biomedical thermometry.

KEYWORDS: *sensor, molecular rotor, paraffin wax, thermometry, biometric identification*

INTRODUCTION

Temperature is an important parameter that may serve as an indicator for predetermination of the physical state of substances. A variety of fluorescent thermo-indicators based on organic, polymeric, and organometallic compounds have been developed for accurate and convenient measurement of temperature.[1−4] The fluorescence (FL) of these compounds is significantly affected by temperature and, in most cases, there is a linear functional relationship between temperature and the FL emission intensity or wavelength. Some polymer solutions and blends that undergo gel-to-solution phase transition exhibit critical optical changes at a certain temperature.[5−8] These sensory materials have long been developed for optical switching and logic-gate functions.[9−12] Some of them have recently achieved an intracellular thermometry in biological and medical applications.[13−19] However, these unique properties and advanced functions have been limited to specifically designed polymers. More convenient and universal sensory systems are still urgently required to amplify and clearly discriminate the optical signals at a certain temperature in order to advance their applications.

Paraffin waxes (PWs) are phase-change materials with the ability to reversibly store and release large amounts of latent heat in the thermal energy management of natural heat sources and waste heat.[20] PWs melt and crystallize at critical temperatures with significant changes in their viscosity (η) and volume (V). With increase in temperature in the molten state, η decreases, tending toward 0, and V increases, tending toward ∞. In contrast, in the crystal state, η increases to ∞ and V decreases to a minimum. These physical changes in η and V may be manifest as optical signals with the aid of optically functional materials. Changes in the FL emission of molecular

Received: May 4, 2015
Accepted: June 12, 2015
Published: June 12, 2015

DOI: 10.1021/acsami.5b03842
ACS Appl. Mater. Interfaces 2015, 7, 14485−14492

rotors (MRs) with twisted molecular structures can be induced by changes in the η of a medium because of the relaxation of the torsional angle in solution.[21−23]

Recently, several fluorescent MRs with η-sensing function have been developed, affording numerous benefits such as easy applicability, high sensitivity, and utility in high spatial/temporal resolution imaging.[24−28] Although these viscosity sensor systems generally function with high accuracy, their application has been limited to the fluids in which the sensor compounds dissolve.[29−31] PWs have a wide range of melting (T_m) and crystallization (T_c) temperatures based on their molecular weights, whereas the solubility parameter is independent of molecular weight. Thus, in hybrid materials combining MRs with PWs, the MRs may exhibit critical FL changes at the phase-transition temperatures of the PWs. However, the conventional MRs mentioned above may not dissolve in PWs owing to the significant differences in the polarity and solubility parameter between the MRs and PWs. Thus, to achieve dissolution of such MRs in PWs, the basic principle "like-dissolves-like" should be considered in the molecular design of the MRs.

In a previous study, the polydiphenylacetylene (PDPA)-derivative pC1 shown in Figure 1 was found to be highly

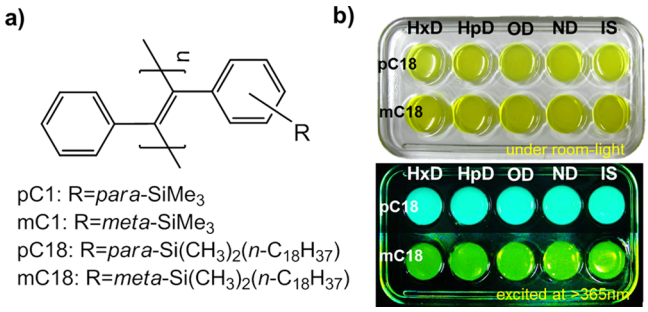

Figure 1. (a) Chemical structures of PDPA derivatives and (b) features of PDPAs dissolved in molten PWs (HxD: hexadecane; HpD: heptadecane; OD: octadecane; ND: nonadecane; IS: icosane) under room light and UV irradiation.

sensitive to the η of various media in the swollen state due to the scissoring and torsion angle relaxation in the intramolecular stack structure.[32−38] The FL emission gradually increased with an increase in η of the media, as could be described by a correlation function. Moreover, hybrid films formed by incorporation of certain molten PWs into pC1 in situ by the swelling method exhibited critical FL changes during the phase-change process.[39] This type of polymer can be termed a fluorescent MR polymer. However, pC1 still did not dissolve in the PWs owing to higher aromatic ratio in the molecular structure. The ratio of PWs incorporated into the pC1 film was limited to several tens wt %. Other PDPAs containing long alkyl chains such as the octadecyl group (pC18 and mC18 in Figure 1) were also synthesized in a previous study.[40−42] The long alkyl side chains efficiently plasticized the glassy-state amorphous PDPA derivative polymers, resulting in very unusual conjugated polymer gums at room temperature, and further enhanced the solubility in nonpolar solvents such as hydrocarbons.[43] This is suggestive of high miscibility between the polymers and PWs.

In this study, the two octadecyl-coupled PDPAs dissolved in molten PWs even up to more than 5 wt % concentrations to produce transparent liquids in the molten state. These PDPAs dissolved in the PWs (hereafter referred to as PDPA-in-PWs) had almost the same phase-transition enthalpies as those of the pure PWs, suggesting that the polymer in the PW does not act as an impurity affecting the phase-transition behavior of the PWs. The PDPA-in-PWs exhibited a critical change in the FL intensity at the T_m and T_c of the PWs. Fluorescent wax papers with desirable features were developed by impregnation of common filter paper with the PDPA-in-PWs to enhance their mechanical integrity and cyclic stability during repeated use. The PDPA-in-PWs were also incorporated into urea capsules by interfacial polymerization using tubular microfluidics. The critical changes in FL emission facilitated various sensor applications in thermometric and biometric identification using the wax papers. Herein, we describe the details of the preparation, thermo-dynamic phase-change properties, and FL responses of the PDPA-in-PWs. Various applications using these materials as novel FL phase-change systems are also suggested.

EXPERIMENTAL SECTION

Materials. The PDPA derivatives of pC1, mC1, pC18, and mC18 were synthesized according to previously reported methods.[40−43] The PDPA derivatives used in this study had high average molecular weights (M_w) of 13.4×10^5, 11.7×10^5, 8.70×10^5, and 8.10×10^5 g mol^{-1} and polydispersity indices (PDI = M_w/M_n) of 1.2, 1.3, 1.4, and 1.6, respectively. All polymers were thoroughly purified by sequential Soxhlet extraction with methanol and acetone. All paraffin waxes (purities: HxD: hexadecane; OD: octadecane; IS: icosane >98.0%; HpD: heptadecane; ND: nonadecane; > 99%) were purchased from TCI in Japan (Tokyo Chemical Industry Co., Ltd.). Filter paper was purchased from ADVANTEC Co., Ltd., Taiwan.

Preparation of Fluorescent Wax Papers. pC18 and mC18 were dissolved in molten PWs (concentration ≈1.0 wt %) and the solutions were spread on top of filter papers at 50 °C and left undisturbed for 10 min. Excess paraffin wax residue was removed simply by treatment with oil adsorption pads (Yuhan Kimberly, Ltd.) for 1 h.

Preparation of Fluorescent Miscrocapsules. Sodium dodecyl sulfate (SDS), poly(vinyl alcohol) (PVA, M_n = 85 000−146 000 g mol^{-1}, 96% hydrolyzed), tetraethylene−pentamine (TEPA), isophorone diisocyanate (IPDI), and dibutyltin dilaurate (DBTDL) were purchased from Sigma-Aldrich and used as received. Ultrapure water (resistivity >18.2 MΩ cm, Purelab Option−Q, ELGA, USA) was degassed and used for all experiments. A 1-mL glass syringe (Hamilton, USA, i.d. = 4.61 mm) was used to inject the discontinuous phase and a 30-mL disposable plastic syringe (HSW, NORM-JECT, Germany, i.d. = 22.9 mm) was used for introduction of the continuous phase. The tubular microfluidic device was assembled by inserting a 30 G needle (NanoNC, Korea) into a Tygon microbore tubing (Saint-Gobain PPL, France, i.d. = 515 μm).[44] The flow rates of the two solutions were independently controlled in a coflow regime using two high-precision infusion pumps (Legato 200, KD Scientific, USA). In the representative preparation of the fluorescent microcapsules, the flow rates of the two pumps were fixed at 1.0 μL s^{-1} and 50 nL s^{-1} for the continuous (aqueous) and discontinuous (organic mixture) phases, respectively. The continuous phase comprised a mixture of water (94 wt %), SDS (2 wt %), PVA (2 wt %), and TEPA (2 wt %). For the discontinuous phase, mC18-in-HxD (2.5 wt % mC18) and IPDI were mixed in mass ratios of 1.5:0.5. DBTDL (0.2 wt %) was added to the discontinuous phase to achieve complete polycondensation between IPDI and TEPA. At the tip of the needle, the organic phase broke into spherical monodisperse droplets in an aqueous mixture to produce an oil-in-water (O/W) emulsion. The O/W droplets were then partially solidified by polycondensation along the tubing length and finally received in a collecting reservoir to perform the remainder of the polycondensation.

Measurements. The weight-average molecular weight (M_w) and number-average molecular weight (M_n) of the PDPA derivatives were

DOI: 10.1021/acsami.5b03842
ACS Appl. Mater. Interfaces 2015, 7, 14485−14492

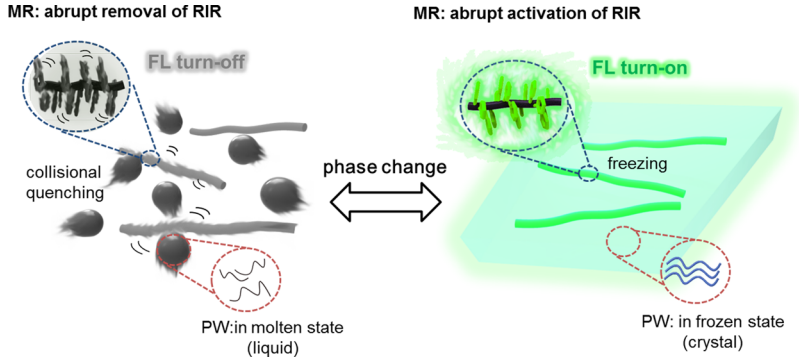

Figure 2. Schematic of phase transition of conceptual MR-in-PW system.

evaluated using gel permeation chromatography (GPC, Shimadzu A10 instruments, Polymer Laboratories, PLgel Mixed-B (300 mm long) column, and HPLC-grade tetrahydrofuran (as an eluent at 40 °C), based on calibration with polystyrene standards. The variable-temperature FL emission spectra were recorded on a JASCO FP-6500 spectrofluorometer equipped with a JASCO ETC-273 temperature controller at an excitation wavelength of 420 nm and a scanning rate of 1000 nm min^{-1}. The heating and cooling rates were both set to 1 °C min^{-1}. Fluorescence images and videos were recorded with a digital camera (Cannon PowerShot A2000 IS) under UV irradiation at an excitation wavelength of >365 nm. Differential scanning calorimetry (DSC; SETARAM DSC141-evo) was performed under pure nitrogen gas with the heating and cooling rates both set to 10 °C min^{-1}. Polarized and FL microscope images were recorded on a Nikon Eclipse E600 fluorescence optical microscope equipped with a Nikon DS-Fi1 digital camera and a superhigh-pressure 100-W Hg lamp (OSRAM, HBO103*W*/2).

RESULTS AND DISCUSSION

The restriction of intramolecular rotation (RIR) of MRs in the condensed state, such as in crystals and aggregates, often leads to enhanced FL emission by eliminating the FL quenching due to solvent collision, vibrational relaxation, and internal conversion, which are deactivation pathways that are operative in the solution state.[45,46] In the case of the current PDPA derivative, the nanosized aggregates suddenly produced by precipitation of the polymer into water exhibited an extremely high FL quantum yield due to the RIR, in contrast with the usual FL quenching of conjugated polymers in aggregates.[47] Such a sudden FL emission enhancement may be the ultimate optical change related to RIR because, in the solution state, the degree of RIR should vary gradually instead of changing abruptly with temperature-induced variation of η of the medium, merely leading to a proportional variation of the FL emission. The ultimate goal of this study is to develop new thermoresponsive sensor systems that exhibit a critical FL change at a certain temperature. To achieve this goal, we conceptualized a system combining MRs and PWs as illustrated as Figure 2. In this concept, the FL emission of the MRs is critically enhanced due to abrupt activation of RIR when the PW undergoes a liquid-to-crystal phase change; the FL emission is again quickly quenched due to abrupt removal of RIR during the reverse crystal-to-liquid change. On the basis of this scheme, we examined the utility of PWs as phase-change media and PDPA derivatives as MRs. C16−C20 hydrocarbons (HxD, HpD, OD, ND, IS in Figure 1) were utilized as the PWs. The two octadecyl-coupled PDPAs (pC18 and mC18 in Figure 1) were selected as MRs. These polymers dissolved very well in all of the molten PWs despite their high molecular weights and rigid backbones; this solubility is due to the high miscibility between the paraffin-like alkyl side chains and the PWs, and gave rise to highly transparent liquids in the molten state. No phase separation between the polymer and paraffin occurred during repeated melting and crystallization. On the other hand, the PDPA congeners containing short alkyl chains (pC1 and mC1 in Figure 1) did not dissolve in the molten PWs.

The thermodynamic properties of the PDPA-in-PWs were evaluated using differential scanning calorimetry (DSC). Table 1 summarizes the enthalpy and critical temperatures of phase transition of the pC18-in-HxD, mC18-in-HxD, pC18-in-OD, and mC18-in-OD systems compared to those of pure HxD and OD (see Supporting Information (SI) Figure S1 for DSC thermograms). All of the PDPA-in-PWs had a clearly defined T_m (~20 °C for pC18- and mC18-in-HxDs; ~30 °C for pC18- and mC18-in-ODs) and T_c (~13 °C for pC18- and mC18-in-HxDs; ~20 °C for pC18- and mC18-in-ODs); these values were slightly lower than those of the pure PWs. The enthalpies of the PDPA-in-PW systems were extremely high (approximately 200 J g^{-1}) and were almost the same as those of the pure PWs. These results indicate that the polymers did not act as an impurity that prevents phase transition of the PWs.

Table 1. Thermodynamic Properties of PDPA-in-PWs (1 wt % PDPA) and Pure PWs

	properties		
material	melting point T_m (°C)	enthalpy of fusion ΔH_{fus} (J g^{-1})	crystallization point T_c (°C)
pure HxD	21.1(17.9)[a]	193.3(227.5)[a]	15.2
pC18-in-HxD	20.5	191.4	12.7
mC18-in-HxD	20.1	199.8	13.1
pure OD	32.0(28.0)[a]	201.8(241.6)[a]	24.4
pC18-in-OD	30.2	199.5	19.8
mC18-in-OD	30.5	203.7	20.3

[a]Reference values.[48,49]

A unique FL response was exhibited by the PDPA-in-PWs during the heating and cooling process. The FL emission spectra of pC18-in-OD and mC18-in-OD are shown in Figure 3. During heating over the temperature range of 10−40 °C (at a rate of 1 °C min^{-1}), the FL intensity declined abruptly (to approximately one-third of the original FL) within a very narrow temperature range of 27.5−30 °C due to endothermic volume expansion of OD (Figure 3a, c). Conversely, a significant enhancement of the FL was observed during the

DOI: 10.1021/acsami.5b03842
ACS Appl. Mater. Interfaces 2015, 7, 14485−14492

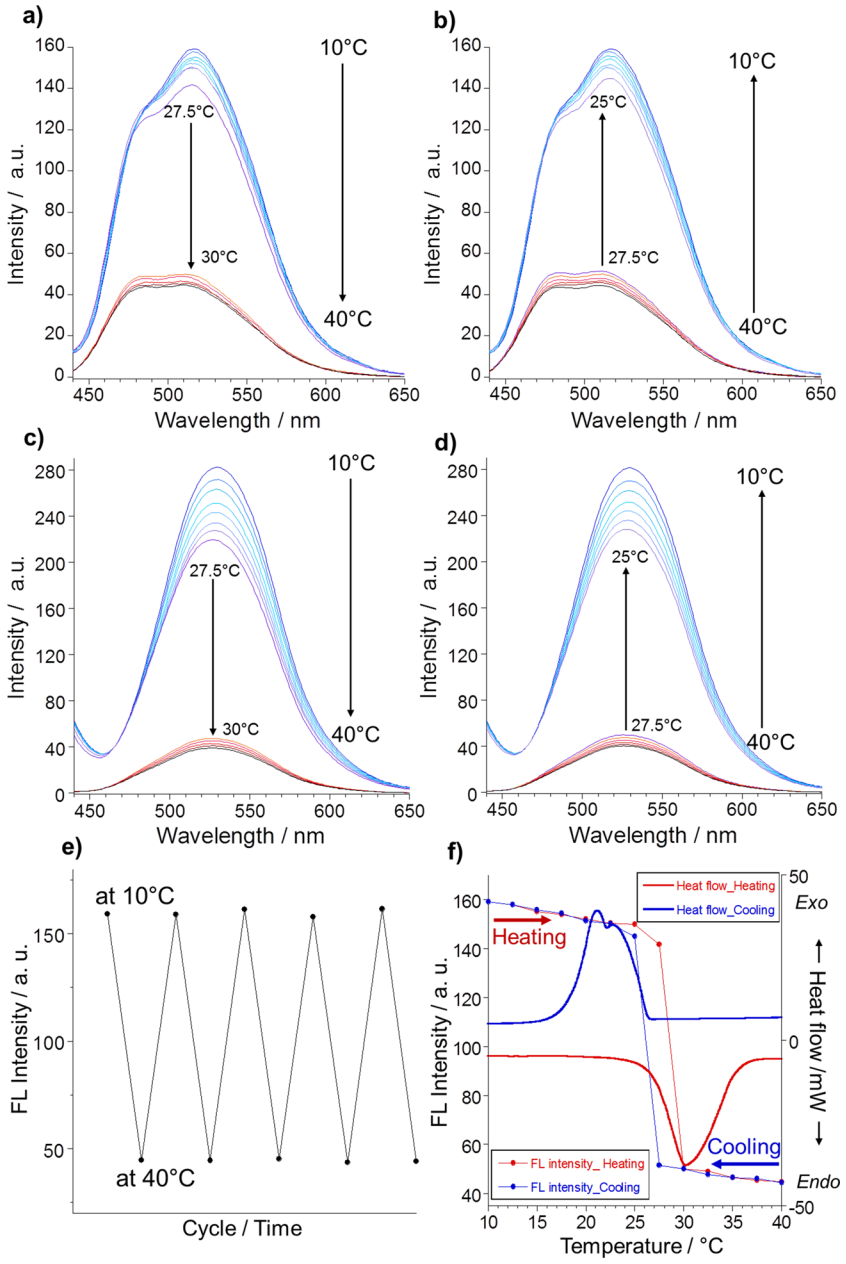

Figure 3. FL emission spectra of 1 wt % pC18-in-OD (a, b) and 1 wt % mC18-in-OD (c, d) during heating (a, c) and cooling (b, d) over the temperature range of 10−40 °C (at a rate of 1 °C min^{-1}). (e) FL intensity of pC18-in-OD during 5 heating (at 40 °C) and cooling (at 10 °C) cycles (excited at 420 nm, monitored at FL maximum wavelength), and (f) comparative variation of FL intensity and heat flow of pC18-in-OD upon heating and cooling (excited at 420 nm, monitored at FL maximum wavelength).

exothermic volume contraction upon cooling from 27.5 to 25 °C (Figure 3b, d). The concentration of the polymer in the PWs and the type of PW did not affect the FL response behavior (SI Figures S2, S3). This critical variation in the FL emission was entirely reversible upon repeated temperature cycling (Figure 3e). The temperature range over which the critical change in FL intensity occurred was congruent with the phase-change temperature observed from DSC analysis (Figure 3f, SI Figure S4). For comparison with the PDPA-in-PW systems, the PDPAs were dissolved in a paraffin mixture (commercial paraffin oil) having no phase transition over a wide temperature range of 10−100 °C. These PDPA-in-paraffin oil systems exhibited a monotonous decrease and increase of the FL intensity upon heating and cooling, respectively (SI Figure S5). This corroborates the postulation that the RIR of the MR should be significantly influenced by the crystal-to-liquid phase transition, whereas in the solution state, the RIR is gradually attenuated based on temperature-induced variation of the viscosity. This suggests that the present MR-in-PW systems should be applicable to thermoresponsive sensors showing a critical optical change.

The unique heat-sensitive FL response of the present MR-in-PW systems enabled their application in thermometry, e.g., write/erase sensor and array-type thermo-indicator systems. To confer mechanical integrity to these systems, the PDPA-in-PWs were impregnated into common filter papers by absorption in the molten sate to provide fluorescent wax papers with good features (SI Figure S6). When the fluorescent wax papers were fully cooled in advance and the entire surface of the paper was held at 27 °C and then brought into contact with a warmed

DOI: 10.1021/acsami.5b03842
ACS Appl. Mater. Interfaces 2015, 7, 14485−14492

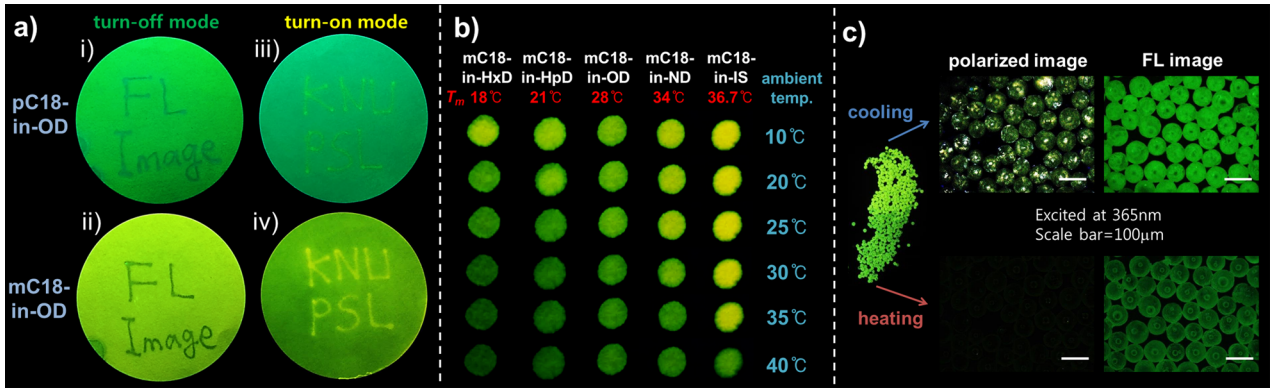

Figure 4. (a) FL imaging (character writing) on wax papers made from pC18-in-OD and mC18-in-OD: (i), (ii) FL turn-off imaging, (iii), (iv) FL turn-on imaging. (b) Array-type thermo-indicator system (five spots were arrayed on the same filter paper by simply depositing each mC18-in-PW). (c) Features of microcapsules made with mC18-in-HxD and corresponding polarized and FL microscope images.

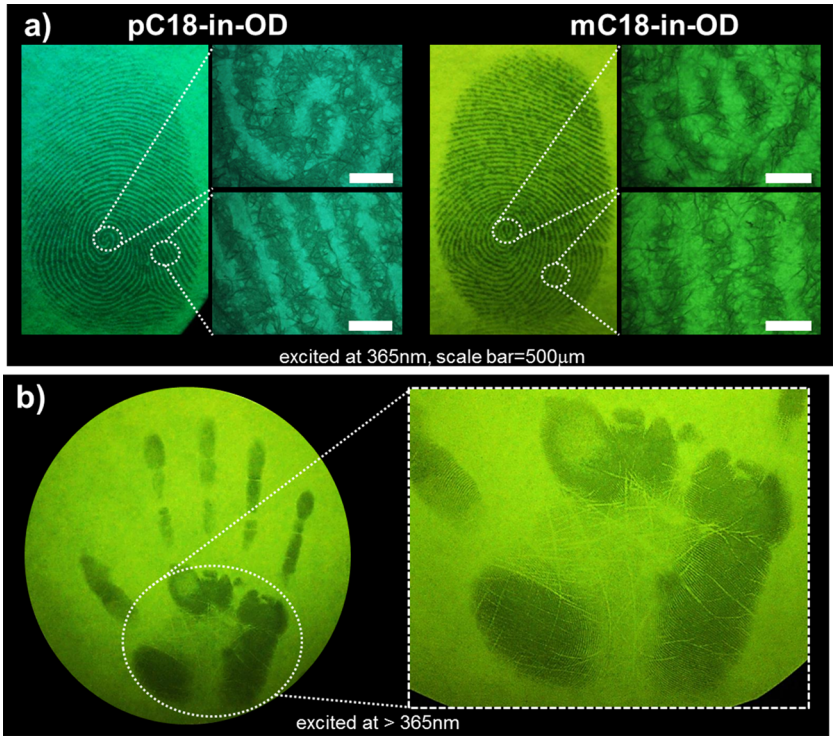

Figure 5. (a) Fingerprint acquisition using FL wax papers made from 1 wt % pC18-in-OD and mC18-in-OD and (b) palmprint acquisition using mC18-in-OD FL wax paper for biometric identification.

metal rod, visually observable FL characters could be imprinted on the paper as a turn-off system (Figure 4a, SI Movies S1 and S2). Subsequently, when the paper was cooled again over the same area, the FL character images could be erased. Conversely, distinctive character images were obtained as a turn-on mode when the fluorescent wax papers were warmed in advance and maintained at 27 °C and then touched with a cooled metal rod (Figure 4a, SI Movies S3 and S4). The FL images could be erased by reheating the paper over the entire region. Moreover, when all mC18-in-PWs (HxD, HpD, OD, ND, IS) with different T_ms were deposited onto the same filter paper as a platform sensor array, changes in the ambient temperature could be recognized by FL evolution at the location of each mC18-in-PW (Figure 4b, SI Movie S5). This type of sensor-array system functions as a specific litmus-type FL thermo-indicator for prospective measurement of multicritical temperatures.

As mentioned above, impregnation of the PDPA-in-PWs into the porous filter paper was successfully achieved by absorption and the waxed paper was resistant to repeated heating and cooling without significant leakage. However, encapsulation of the PWs may be a more useful method for enhancing their mechanical integrity and cyclic stability during repeated use.[50−53] By employing reported methods,[54] the molten-state mC18-in-HxD at room temperature was encapsulated into polyurea by interfacial polymerization using tubular microfluidics to give well-featured fluorescent microcapsules (Figure 4c). Similar to the fluorescent wax paper, these capsules also showed critical changes in the FL emission at the phase-transition temperatures (T_m and T_c) of HxD (see Figure 4c and SI Figure S7 for the FL emission spectra).

DOI: 10.1021/acsami.5b03842
ACS Appl. Mater. Interfaces 2015, 7, 14485−14492

The application of the present MR-in-PW systems was further extended to biometric identification. Normal body temperature is maintained at about 36.5 °C, which is higher than the T_m (~30 °C) of the PDPA-in-ODs. Hence, it was envisioned that the PDPA-in-OD systems could potentially be used for fingerprint recognition.[55,56] When the fluorescent wax papers of PDPA-in-ODs were held at room temperature and brought into contact with the human body, the FL emission was immediately attenuated due to melting of the OD. Notably, when the fluorescent paper was touched softly with a finger, a high-resolution FL image of the fingerprint could easily be observed under irradiation with a common ultraviolet lamp (Figure 5a, SI Movies S6 and S7). Notably, once the fingerprinting was done, the FL image was semipermanently retained at room temperature owing to the extremely high phase-transition enthalpy of OD (SI Figure S8). Moreover, the fingerprint image was erased during the heating/cooling cycle and could be regenerated by touching the paper again. This fingerprinting could be repeated almost unlimitedly. Our preliminary demonstrations suggest the potential applicability of the present MR-in-PW hybrid as a fingerprint identification system. In addition, it was easy to prepare larger fluorescent wax papers that facilitated high-resolution FL imaging of a palmprint on the paper (Figure 5b). The present sensor system responds to body heat, which is a sensing mechanism that is completely different from that of conventional reflectance-based fingerprint sensors.[57] This new approach should prove effective for preventing falsification of fingerprints made from gelatin or silicones, thereby providing an enhanced security feature.[58−60] As a matter of course, the fluorescent wax papers of PDPA-in-paraffin oil were not effective for FL image patterning and fingerprinting owing to the lack of thermal storage capacity of paraffin oil (SI Movie S8).

CONCLUSIONS

A new thermoresponsive sensor system comprising MRs and PWs was developed. Coupled PDPAs with long alkyl chains were used as MRs; these PDPAs dissolved very well in the molten PWs. The polymers did not act as an impurity that prevents phase transition of the PWs. The enthalpies and phase-transition temperatures of the present PDPA-in-PW systems were almost the same as those of the pure PWs, and thus the PDPA-in-PW systems exhibited critical FL variations during phase transition. The present MR-in-PW systems were impregnated into common filter paper by absorption or were encapsulated into urea resin to enhance their mechanical integrity and cyclic stability during repeated use. The wax papers could be utilized in highly advanced applications, including thermometric and biometric identification applications. Investigations to find novel MRs and phase-change materials and then to combine the two functional materials as a single-component material via covalent bonding are now underway in our laboratory. Our findings should be helpful in designing new thermoresponsive FL phase-change systems for further advanced applications.

ASSOCIATED CONTENT

Supporting Information

DSC thermograms, FL emission spectra, microscopy images (Figures S1−S8), and supplementary movies (Movies S1−S8). The Supporting Information is available free of charge on the ACS Publications website at DOI: 10.1021/acsami.5b03842.

AUTHOR INFORMATION

Corresponding Author

*E-mail: gkwak@knu.ac.kr.

Notes

The authors declare no competing financial interest.

ACKNOWLEDGMENTS

This work was supported by the Basic Science Research Program through the National Research Foundation of Korea (NRF) grants funded by the Korea government (MEST) (2014R1A2A1A11052446).

REFERENCES

(1) Yan, D.; Lu, J.; Ma, J.; Wei, M.; Evans, D. G.; Duan, X. Reversibly Thermochromic, Fluorescent Ultrathin Films with a Supramolecular Architecture. *Angew. Chem., Int. Ed.* **2011**, *50*, 720−723.

(2) Feng, J.; Tian, K.; Hu, D.; Wang, S.; Li, S.; Zeng, Y.; Li, Y.; Yang, G. A Triarylboron-Based Fluorescent Thermometer: Sensitive Over a Wide Temperature Range. *Angew. Chem., Int. Ed.* **2011**, *50*, 8072−8076.

(3) Cauzzi, D.; Pattacini, R.; Delferro, M.; Dini, F.; Natale, C. D.; Paolesse, R.; Bonacchi, S.; Montalti, M.; Zaccheroni, N.; Calvaresi, M.; Zerbetto, F.; Prodi, L. Temperature-Dependent Fluorescence of Cu5Metal Clusters: A Molecular Thermometer. *Angew. Chem., Int. Ed.* **2012**, *51*, 9662−9665.

(4) Uchiyama, S.; de Silva, A. P.; Iwai, K. Luminescent Molecular Thermometers. *J. Chem. Educ.* **2006**, *83*, 720−727.

(5) Balamurugan, S. S.; Bantchev, G. B.; Yang, Y.; McCarley, R. L. Highly Water-Soluble Thermally Responsive Poly(thiophene)-Based Brushes. *Angew. Chem., Int. Ed.* **2005**, *44*, 4872−4876.

(6) Tang, L.; Jin, J. K.; Qin, A.; Yuan, W. Z.; Mao, Y.; Mei, J.; Sun, J. Z.; Tang, B. Z. A Fluorescent Thermometer Operating in Aggregation-Induced Emission Mechanism: Probing Thermal Transitions of PNIPAM in Water. *Chem. Commun.* **2009**, 4974−4976.

(7) Gota, C.; Uchiyama, S.; Yoshihara, T.; Tobita, S.; Ohwada, T. Temperature-Dependent Fluorescence Lifetime of a Fluorescent Polymeric Thermometer, Poly(N-isopropylacrylamide), Labeled by Polarity and Hydrogen Bonding Sensitive 4-Sulfamoyl-7-amino-benzofurazan. *J. Phys. Chem. B* **2008**, *112*, 2829−2836.

(8) Uchiyama, S.; Matsumura, Y.; de Silva, A. P.; Iwai, K. Modulation of the Sensitive Temperature Range of Fluorescent Molecular Thermometers Based on Thermoresponsive Polymers. *Anal. Chem.* **2004**, *76*, 1793−1798.

(9) Uchiyama, S.; Kawai, N.; de Silva, A. P.; Iwai, K. Fluorescent Polymeric AND Logic Gate with Temperature and pH as Inputs. *J. Am. Chem. Soc.* **2004**, *126*, 3032−3033.

(10) Guo, Z.; Zhu, W.; Xiong, Y.; Tian, H. Multiple Logic Fluorescent Thermometer System Based on N-Isopropylmethacrylamide Copolymer Bearing Dicyanomethylene-4H-pyran Moiety. *Macromolecules* **2009**, *42*, 1448−1453.

(11) Pietsch, C.; Schubert, U. S.; Hoogenboom, R. Aqueous Polymeric Sensors Based on Temperature-Induced Polymer Phase Transitions and Solvatochromic Dyes. *Chem. Commun.* **2011**, *47*, 8750−8765.

(12) Guo, Z.; Zhu, W.; Tian, H. Dicyanomethylene-4H-pyran Chromophores for OLED Emitters, Logic Gates and Optical Chemosensors. *Chem. Commun.* **2012**, *48*, 6073−6084.

(13) Okabe, K.; Inada, N.; Gota, C.; Harada, Y.; Funatsu, T.; Uchiyama, S. Quantitative Determination of Ecdysteroids in Sida rhombifolia L. and various other Sida Species Using LC-UV, and their Anatomical Characterization. *Nat. Commun.* **2012**, *3*, 705−713.

(14) Jaque, D.; del Rosal, B.; Rodriquez, E. M.; Maestro, L. M.; Haro-Gonzalez, P.; Sole, J. G. Fluorescent Nanothermometers for Intracellular Thermal Sensing. *Nanomedicine* **2014**, *9*, 1047−1062.

(15) Shang, L.; Stockmar, F.; Azadfar, N.; Nienhaus, G. U. Intracellular Thermometry by Using Fluorescent Gold Nanoclusters. *Angew. Chem., Int. Ed.* **2013**, *52*, 11154−11157.

DOI: 10.1021/acsami.5b03842
ACS Appl. Mater. Interfaces 2015, 7, 14485−14492

(16) Tsuji, T.; Yoshida, S.; Yoshida, A.; Uchiyama, S. Cationic Fluorescent Polymeric Thermometers with the Ability to Enter Yeast and Mammalian Cells for Practical Intracellular Temperature Measurements. *Anal. Chem.* **2013**, *85*, 9815−9823.
(17) Gota, C.; Okabe, K.; Funatsu, T.; Harada, Y.; Uchiyama, S. Hydrophilic Fluorescent Nanogel Thermometer for Intracellular Thermometry. *J. Am. Chem. Soc.* **2009**, *131*, 2766−2767.
(18) Wang, Z.; Chen, S.; Lam, J. W. Y.; Qin, W.; Kwok, R. T. K.; Xie, N.; Hu, Q.; Tang, B. Z. Long-Term Fluorescent Cellular Tracing by the Aggregates of AIE Bioconjugates. *J. Am. Chem. Soc.* **2013**, *135*, 8238−8245.
(19) Chen, Y.; Lam, J. W. Y.; Chen, S.; Tang, B. Z. Synthesis, Properties, and Applications of Poly(ethylene glycol)-Decorated Tetraphenylethenes. *J. Mater. Chem. C* **2014**, *2*, 6192−6198.
(20) Pielichowska, K.; Pielichowski, K. Phase Change Materials for Thermal Energy Storage. *Prog. Mater. Sci.* **2014**, *65*, 67−123.
(21) Loutfy, R. O.; Law, K. Y. Electrochemistry and Spectroscopy of Intramolecular Charge-Transfer Complexes. p-N,N-Dialkylaminobenzylidenemalononitriles. *J. Phys. Chem.* **1980**, *84*, 2803−2808.
(22) Loutfy, R. O.; Arnold, B. J. Effect of Viscosity and Temperature on Torsional Relaxation of Molecular Rotors. *J. Phys. Chem.* **1982**, *86*, 4205−4211.
(23) Allen, B. D.; Benniston, A. C.; Harriman, A.; Rostron, S.; Yu, C. The Photophysical Properties of a Julolidene-Based Molecular Rotor. *Phys. Chem. Chem. Phys.* **2005**, *7*, 3035−3040.
(24) Haidekker, M. A.; Brady, T. P.; Lichlyter, D.; Theodorakis, E. A. A Ratiometric Fluorescent Viscosity Sensor. *J. Am. Chem. Soc.* **2006**, *128*, 398−399.
(25) Fischer, D.; Theodorakis, E. A.; Haidekker, M. A. Synthesis and Use of an In-Solution Ratiometric Fluorescent Viscosity Sensor. *Nat. Protoc.* **2007**, *2*, 227−236.
(26) Ghiggino, K. P.; Hutchison, J. A.; Langford, S. J.; Latter, M. J.; Lee, M. A. P.; Lowenstern, P. R.; Scholes, C.; Takezaki, M.; Wilman, B. E. Porphyrin-Based Molecular Rotors as Fluorescent Probes of Nanoscale Environments. *Adv. Funct. Mater.* **2007**, *17*, 805−813.
(27) Zhu, D.; Haidekker, M. A.; Lee, J.-S.; Won, Y.-Y.; Lee, J. C.-M. Application of Molecular Rotors to the Determination of the Molecular Weight Dependence of Viscosity in Polymer Melts. *Macromolecules* **2007**, *40*, 7730−7732.
(28) Kuimova, M. K.; Botchway, S. W.; Parker, A. W.; Balaz, M.; Collins, H. A.; Anderson, H. L.; Suhling, K.; Ogilby, P. R. Imaging Intracellular Viscosity of a Single Cell During Photoinduced Cell Death. *Nat. Chem.* **2009**, *1*, 69−73.
(29) Haidekker, M. A.; Brady, T. P.; Linchlyter, D.; Theodorakis, E. A. Effects of Solvent Polarity and Solvent Viscosity on the Fluorescent Properties of Molecular Rotors and Related Probes. *Bioorg. Chem.* **2005**, *33*, 415−425.
(30) Haidekker, M. A.; Akers, W. J.; Fischer, D.; Theodorakis, E. A. Optical Fiber-Based Fluorescent Viscosity Sensor. *Opt. Lett.* **2006**, *31*, 2529−2531.
(31) Lichlyter, D. J.; Haidekker, M. A. Immobilization Techniques for Molecular Rotors-Towards a Solid-State Viscosity Sensor Platform. *Sens. Actuators, B* **2009**, *139*, 648−656.
(32) Kwak, G.; Lee, W.-E.; Jeong, H.; Sakaguchi, T.; Fujiki, M. Swelling-Induced Emission Enhancement in Substituted Acetylene Polymer Film with Large Fractional Free Volume: Fluorescence Response to Organic Solvent Stimuli. *Macromolecules* **2009**, *42*, 20−24.
(33) Kwak, G.; Lee, W.-E.; Kim, W.-H.; Lee, H. Fluorescence Imaging of Latent Fingerprints on Conjugated Polymer Films with Large Fractional Free Volume. *Chem. Commun.* **2009**, 2112−2114.
(34) Lee, W.-E.; Lee, C.-L.; Sakaguchi, T.; Fujiki, M.; Kwak, G. Fluorescent Viscosity Sensor Film of Molecular-Scale Porous Polymer with Intramolecular π-Stack Structure. *Macromolecules* **2011**, *44*, 432−436.
(35) Jeong, H.; Lee, W.-E.; Kwak, G. Enhancements in Emission and Chemical Resistance of Substituted Acetylene Polymer via in Situ Sol-Gel Reaction in Film. *Macromolecules* **2010**, *43*, 1152−1155.
(36) Park, H.; Han, D.-C.; Han, D.-H.; Kim, S.-J.; Lee, W.-E.; Kwak, G. Emission Enhancement, Photooxidative Stability, and Fluorescence Image Patterning of Conjugated Polymer Film via in Situ Hybridization with UV-Curable Acrylate Monomers. *Macromolecules* **2011**, *44*, 9351−9355.
(37) Lee, W.-E.; Jin, Y.-J.; Park, L.-S.; Kwak, G. Fluorescent Actuator Based on Microporous Conjugated Polymer with Intramolecular Stack Structure. *Adv. Mater.* **2012**, *24*, 5604−5609.
(38) Kim, S.-I.; Jin, Y.-J.; Lee, W.-E.; Yu, R.; Park, S.-J.; Kim, H.-J.; Song, K.-H.; Kwak, G. Microporous Conjugated Polymers with Enhanced Emission in Immiscible Two-Phase System in Response to Surfactants. *Adv. Mater. Interfaces* **2014**, *1*, 1300029(1)−1300029(7).
(39) Jin, Y.-J.; Kim, B. S.-I.; Lee, W.-E.; Lee, C.-L.; Kim, H.; Song, K.-H.; Jang, S.-Y.; Kwak, G. Phase-Change Hybrids for Thermo-Responsive Sensors and Actuators. *NPG Asia Mater.* **2014**, *6*, e137−e144.
(40) Kwak, G.; Minaguchi, M.; Sakaguchi, T.; Masuda, T.; Fujiki, M. Poly(diphenylacetylene) Bearing Long Alkyl Side Chain via Silylene Linkage: Its Lyotropic Liquid Crystallinity and Optical Anisotropy. *Chem. Mater.* **2007**, *19*, 3654−3661.
(41) Kwak, G.; Minaguchi, M.; Sakaguchi, T.; Masuda, T.; Fujiki, M. Alkyl Side-Chain Length Effects on Fluorescence Dynamics, Lamellar Layer Structures, and Optical Anisotropy of Poly(diphenylacetylene) Derivatives. *Macromolecules* **2008**, *41*, 2743−2746.
(42) Lee, W.-E.; Kim, J.-W.; Oh, C.-J.; Sakaguchi, T.; Fujiki, M.; Kwak, G. Correlation of Intramolecular Excimer Emission with Lamellar Layer Distance in Liquid-Crystalline Polymers: Verification by the Film-Swelling Method. *Angew. Chem., Int. Ed.* **2010**, *49*, 1406−1409.
(43) Jin, Y.-J.; Bae, J.-E.; Cho, K.-S.; Lee, W.-E.; Hwang, D.-Y.; Kwak, G. Room Temperature Fluorescent Conjugated Polymer Gums. *Adv. Funct. Mater.* **2014**, *24*, 1928−1937.
(44) Lone, S.; Lee, H. M.; Kim, G. M.; Koh, W.-G.; Cheong, I. W. Facile and Highly Efficient Microencapsulation of a Phase Change Material Using Tubular Microfluidics. *Colloids Surf., A* **2013**, *422*, 61−67.
(45) Mei, J.; Hong, Y.; Lam, J. W. Y.; Qin, A.; Tang, Y.; Tang, B. Z. Aggregation-Induced Emission: The Whole Is More Brilliant than the Parts. *Adv. Mater.* **2014**, *26*, 5429−5479.
(46) Hong, Y.; Lam, J. W. Y.; Tang, B. Z. Aggregation-Induced Emission: Phenomenon, Mechanism and Applications. *Chem. Commun.* **2009**, 4332−4353.
(47) Kim, B. S.-I.; Jin, Y.-J.; Lee, W.-E.; Byun, D. J.; Yu, R.; Park, S.-J.; Kim, H.; Song, K.-H.; Jang, S.-Y.; Kwak, G. Highly Fluorescent, Photostable, Conjugated Polymer Dots with Amorphous, Glassy-State, Coarsened Structure for Bioimaging. *Adv. Opt. Mater.* **2015**, *3*, 78−86.
(48) Barbillon, P.; Schuffenecker, L.; Dellacherie, J.; Balesdent, D.; Dirande, M. Enthalpy Change from 260 to 340 K for all Normal Paraffins from Octadecane (n-C18) to Hexacosane (n-C26). *J. Chim. Phys. Phys.-Chim. Biol.* **1991**, *88*, 91−113.
(49) Parks, G. S.; Moore, G. E.; Renquist, M. L.; Naylor, B. F.; McClaine, L. A.; Fujii, P. S.; Hatton, J. A. Thermal Data on Organic Compounds. XXV. Some Heat-Capacity, Entropy, and Free-Energy Data for Nine Hydrocarbons of High Molecular Weight. *J. Am. Chem. Soc.* **1949**, *71*, 3386−3389.
(50) Kwon, H. J.; Cheong, I. W.; Kim, J. H. Preparation of n-octadecane Nanocapsules by Using Interfacial Redox Initiation in Miniemulsion Polymerization. *Macromol. Res.* **2010**, *18*, 923−926.
(51) Li, B.; Liu, T.; Hu, L.; Wang, Y.; Gao, L. Fabrication and Properties of Microencapsulated Paraffin@SiO_2 Phase Change Composite for Thermal Energy Storage. *ACS Sustainable Chem. Eng.* **2013**, *1*, 374−380.
(52) Hong, Y.; Ding, S.; Wu, W.; Hu, J.; Voevodin, A. A.; Gschewender, L.; Snyder, E.; Chow, L.; Su, M. Enhancing Heat Capacity of Colloidal Suspension Using Nanoscale Encapsulated Phase-Change Materials for Heat Transfer. *ACS Appl. Mater. Interfaces* **2010**, *2*, 1685−1691.
(53) Phadungphatthanakoon, S.; Poompradub, S.; Wanichwecharungruang, S. P. Increasing the Thermal Storage

DOI: 10.1021/acsami.5b03842
ACS Appl. Mater. Interfaces 2015, 7, 14485−14492

Capacity of a Phase Change Material by Encapsulation: Preparation and Application in Natural Rubber. *ACS Appl. Mater. Interfaces* **2011**, *3*, 3691−3696.
(54) Park, S.; Lee, Y.; Kim, Y. S.; Lee, H. M.; Kim, J. H.; Cheong, I. W.; Koh, W.-G. Magnetic Nanoparticle-Embedded PCM Nanocapsules Based on Paraffin Core and Polyurea Shell. *Colloids Surf., A* **2014**, *450*, 46−51.
(55) Unar, J. A.; Seng, W. C.; Abbasi, A. A Review of Biometric Technology Along with Trends and Prospects. *Pattern Recognit.* **2014**, *47*, 2673−2688.
(56) Bharadwaj, S.; Vatsa, M.; Singh, R. Biometric Quality: A Review of Fingerprint, Iris, and Face. *EURASIP J. Image Video Process.* **2014**, *34*, 1−28.
(57) Maltoni, D.; Maio, D.; Jain, A. K.; Prabhakar, S. *Handbook of Fingerprint Recognition*, 2nd ed.; Springer: London, 2009; pp 57−95.
(58) El-Abed, M.; Lacharme, P.; Rosenberger, C. Privacy and Security Assessment of Biometric Systems. In *Advances in Security and Privacy of Biometric Systems*; Cambridge Scholars Publishing: Newcastle upon Tyne, U.K., 2015.
(59) Xiao, Q. Security Issues in Biometric Authentication. In *Proceedings of the 2005 IEEE Workshop on Information Assurance and Security, United States Military Academy, West Point, NY*; IEEE: New York, 2005; pp 8−13.
(60) Barral, C.; Tria, A. Fake Fingers in Fingerprint Recognition: Glycerin Supersedes Gelatin. In *Formal to Practical Security, Lecture Notes in Computer Science*; series Vol. *5458*; Springer: Berlin Heidelberg, 2009; pp 57−69.

DOI: 10.1021/acsami.5b03842
ACS Appl. Mater. Interfaces 2015, 7, 14485−14492